Eur. Phys. J. B **36**, 209–214 (2003)
DOI: 10.1140/epjb/e2003-00337-6

THE EUROPEAN PHYSICAL JOURNAL B

2-Dimensional polymers confined in a strip

H.-P. Hsu[a] and P. Grassberger[b]

John-von-Neumann Institute for Computing, Forschungszentrum Jülich, 52425 Jülich, Germany

Received 14 August 2003
Published online 8 December 2003 –

Abstract. Single two dimensional polymers confined to a strip are studied by Monte Carlo simulations. They are described by N-step self-avoiding random walks on a square lattice between two parallel hard walls with distance $1 \ll D \ll N^\nu$ ($\nu = 3/4$ is the Flory exponent). For the simulations we employ the pruned-enriched-Rosenbluth method (PERM) with Markovian anticipation. We measure the densities of monomers and of end points as functions of the distance from the walls, the longitudinal extent of the chain, and the forces exerted on the walls. Their scaling with D and the universal ratio between force and monomer density at the wall are compared to theoretical predictions.

PACS. 61.25.Hq Macromolecular and polymer solutions; polymer melts; swelling – 07.05.Tp Computer modeling and simulation – 61.41.+e Polymers, elastomers, and plastics

1 Introduction

The behaviour of flexible polymers in a good solvent confined to different geometries and in the presence of walls or other obstacles have been studied for many years [1,2]. A particularly simple geometry is the space between two parallel walls. For simplicity we shall only discuss here the case of walls without energetic effects, i.e. the walls play a purely geometric role.

An important theoretical prediction is that near such a wall the monomer density profile increases as $z^{1/\nu}$, where z is the distance from the wall ($z \ll D$, and D is the width between the two parallel walls) and ν is the Flory exponent [1]. This should hold in any dimension of space d. On the other hand it is intuitively obvious that the force exerted by the polymer onto the wall is proportional to the monomer density near the wall. The ratio between the two can be expressed in terms of a universal amplitude ratio which has been calculated by Eisenriegler [3] (using *conformal invariance* results of Cardy et al. [4]) in $d = 2$, and in any $d \leq 4$ by Eisenriegler [5] by means of an ϵ-expansion. Attempts to verify these detailed predictions by Monte Carlo simulations in three dimensions [6–9] have so far been without very convincing results. As far as we know, no attempt was made yet to verify them in $d = 2$, and that is where the present paper sets in.

We study single polymer chains confined to a 2-d strip. They are described by self-avoiding random walks (SAWs) of N steps on a square lattice between two hard walls with distance D as shown in Figure 1. More precisely, monomers are supposed to sit on lattice sites and D is the number of rows accessible to monomers, i.e. the walls are placed at $y = 0$ and at $y = D + 1$, and the monomers can be at $y = 1, \ldots D$. We only consider the case where the Flory radius of a free chain of length N, $R_F \approx N^\nu$, is much larger than D. When using a chain growth algorithm, the polymer has then to grow , after a short initial phase of $\sim D^{1/\nu}$ steps, in either the positive or negative x-direction without possibility to change its orientation. This allows us to use an additional wall at $x < x_0$ which forces all chains to grow into the positive x-direction. For $N \gg D^{1/\nu}$ this will essentially reduce the partition sum by a constant factor, without affecting any of the scaling laws or any of the detailed comparisons with theoretical predictions. On the other hand, it simplifies the subsequent discussion.

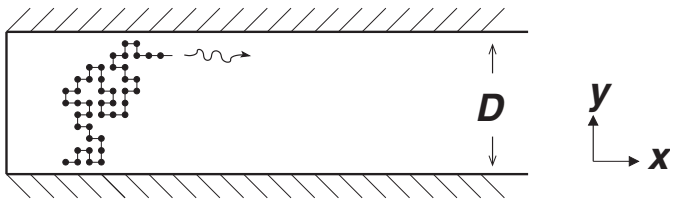

Fig. 1. Schematic drawing of a polymer chain growing inside a strip, and with an additional wall added at $x = 0$. Monomers are only allowed at lattice sites $x > 0$ and $1 \leq y \leq D$.

[a] e-mail: h.p.hsu@fz-juelich.de
[b] e-mail: p.grassberger@fz-juelich.de

The force exerted onto the wall is most straightforwardly expressed in terms of the work done when moving one of the walls, i.e. by the dependence of the free energy – and thus also of the partition sum – on D,

$$F = k_B T \, \frac{\partial \ln Z_N}{\partial D} \, , \tag{1}$$

where we have introduced a dummy temperature T which can take any positive value. The partition sum Z_N is just the number of N-step SAWs in the strip starting from a given x, but summed over all values $1 \le y_0 \le D$ of the y-component of the starting point.

The partition sum of a free SAW in infinite volume scales for $N \to \infty$ as $Z_N = \mu_\infty^{-N} N^{\gamma-1}$ with μ_∞ being the critical fugacity per monomer, and with $\gamma = 43/32$ being a universal exponent. In contrast, the partition function on a strip scales as

$$Z_N \sim \mu_D^{-N} \, , \tag{2}$$

without the power correction and with μ_D scaling for large D as

$$\mu_D - \mu_\infty \approx a D^{-1/\nu} \, . \tag{3}$$

with a being a non-universal amplitude. The force per monomer is then obtained as

$$f = F/N \sim k_B T \; D^{-1-1/\nu} \, . \tag{4}$$

Standard fixed-length Markov Chain Monte Carlo simulations do not give estimates of the partition sum or of the free energy, so that equations (1–4) cannot be used directly. This has led to algorithms specifically designed for estimation of forces [10], but employing the pruned-enriched-Rosenbluth method (PERM) [11] one can use equations (1–4) directly.

Using PERM with k-step Markovian anticipation [12–14], we measured the partition sum directly and estimated the dependence of the monomer fugacity on the width D. In the same simulations also the monomer density profile, the end-to-end distance along the strip, and the density profile of chain ends are measured.

Details of the simulation method are given in the next section, results and their comparison with theoretical predictions are discussed in Section 3.

2 Algorithm: PERM with k-step Markovian anticipation

PERM [11] is a chain growth algorithm with population control. Polymer chains are built like random walks by adding one monomer at each step. We use a Rosenbluth like bias for self-avoidance. As usual, this bias is compensated by a weight factor [15], i.e. each sample configuration should be given a weight. But actually we use a stronger bias which in addition suppresses dense configurations and samples more finely relatively open chain configurations, called *Markovian anticipation* in [13].

In k-step Markovian anticipation, we let the additional bias in the next step depend on the last k steps made before. Let us denote the $2d$ directions on a d-dimensional hypercubic lattice by $s = 0, \ldots, 2d-1$. All possible $(k+1)$-step configurations (k previous steps $i = -1, -2, \ldots -k$ plus one future step $i = 0$) are then indexed by

$$\mathbf{S} = (s_{-k}, \ldots, s_0) = (\mathbf{s}, s_0) \, . \tag{5}$$

In addition, choose an integer $m \approx 100$ (the precise value is not important). Either during an auxiliary run or during the early stages of the present run, we obtained a histogram H_m such that $H_m(\mathbf{S})$ is the accumulated weight at chain length $n+m$ of those chains which had configuration $\mathbf{S}$ during steps $n-k, n-k+1, \ldots n$. Since we sample uniformly, $H_0(\mathbf{S})$ is independent of $\mathbf{S}$. Thus $H_m(\mathbf{S})$ with $m > 0$ indicates how "successful" is a configuration $\mathbf{S}$ after m more steps. In importance sampling we want each chosen direction to have in average the same later success. Therefore we choose the next step with probability

$$p(s_0|\mathbf{s}) = \frac{H_m(\mathbf{s}, s_0)}{\sum_{s_0'=0}^{2d-1} H_m(\mathbf{s}, s_0')} . \tag{6}$$

In our simulations we choose $k = 9$ and $m = 100$. We accumulate contributions to H only for $n + m > 300$, and we apply equation (6) only for chain lengths $> k$ (for chain lengths $< k$ there is not yet enough history to condition upon).

Accumulating the histogram only for $n \gg 1$ is suggested by the fact that only for large n the anisotropic bias is fully developed [13]. This anisotropy makes the histogram strongly dependent on D. We found that using for all D only the histogram obtained for free chains, i.e. for $D = \infty$, gives nearly the same efficiency. This is quite different from the case where the anisotropy is not due to geometry, but is due to stretching of the polymer. In the latter case, simulations with Markovian anticipation become much more efficient with increased stretching [16]. This is not the case for the present problem where the anisotropy is due to geometric constraints, for which PERM with Markovian anticipation is however still the most efficient known simulation method by far.

3 Results

Before presenting our results, let us stress that we have several possibilities for checking our algorithm. For very large D we can compare our estimates of μ with the very precise estimate $\mu_\infty = 0.37905228$ [17,18]. For $D \le 11$ we can compare with exact transfer matrix calculations of [19]. And for $D \le 2$ we can even solve the problem analytically.

For $D = 1$, the polymer can only grow in a straight configuration, giving $\mu_{(D=1)} = 1$. For $D = 2$, each step can be either up (u), down (d), or to the right (r). After an 'u' or 'd' move, the next step has to be 'r', while any move is possible after 'r'. Lumping moves 'u' and 'd' together into a vertical move ('v'), we see that the set of all

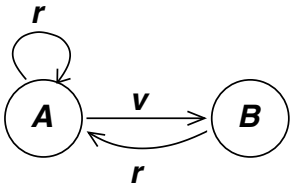

Fig. 2. Graph accepting the regular grammar of vertical ('v') and right ('r') moves for $D = 2$. The node labelled 'A' is the start node [20]. If one wants to distinguish also between 'u' and 'd' moves, the graph is somewhat more complicated and contains also a transient part. This is skipped here for simplicity.

possible configurations forms a regular language [20] with the associated graph shown in Figure 2. The partition sum for chains of length N is just twice the $(N+1)$st Fibonacci number,

$$Z_N(D=2) = 2F_{N+1} \quad (N \geq 1) \; , \tag{7}$$

where $F_0 = F_1 = 1$ and $F_N = F_{N-1} + F_{N-2}$. Thus the critical monomer fugacity for $D = 2$ is the inverse of the golden mean,

$$\mu_{D=2} = g^{-1} \equiv \frac{\sqrt{5}-1}{2} = 0.61803\ldots \tag{8}$$

In this case, we can also show that Markovian anticipation gives the optimal bias. Markovian anticipation corresponds in this case to $p_r : p_v = g : 1$ if a vertical move is allowed, and $p_r : p_v = 1 : 0$ else. This choice leads to weights which oscillate between two values, thus no population control (pruning/cloning) is needed [21]. All this is verified in our simulations, which serves thus as a test for our algorithms.

For $D > 2$, we used simulations. We simulated strip widths up to $D = 320$ and chain length between $N = 3000$ (for $D = 2$) and $N = 125,000$ (for $D = 320$). Critical fugacities are determined by plotting $Z_N \mu_D^N$ against $\log N$ and demanding that these curves become horizontal for large N. Results are shown in Figure 3, where we plot $\mu_D - \mu_\infty$ with $\mu_\infty = 0.37905228$ [18]. They are in perfect agreement with the theoretical prediction of equation (3), and provide the estimate $a = 0.7365 \pm 0.0007$. In addition, μ_D can be compared for $D = 3$ to 12 with the transfer matrix results of [19]. For all D, the values agree for at least six digits.

As we said in the introduction, we expect the force f onto the wall to be proportional to the monomer density $\rho(y)$ near the wall. The precise relation is given by Eisenriegler [5]

$$\lim_{y\to 0} k\frac{\rho(y)}{y^{1/\nu}} = B\frac{f}{k_B T} \; . \tag{9}$$

Here the non-universal amplitude k relates the end-to-end distance of a free SAW to the chain length, $k = R_x^{1/\nu}/N = 0.5297 \pm 0.0002$ [22] for the square lattice. On the other hand, B is a universal number. For ideal chains $B = 2$, while for chains with excluded volume in $4 - \epsilon$ dimensions one has $B \approx 2(1 - b_1\epsilon)$ with $b_1 = 0.075$ [5]. The latter is

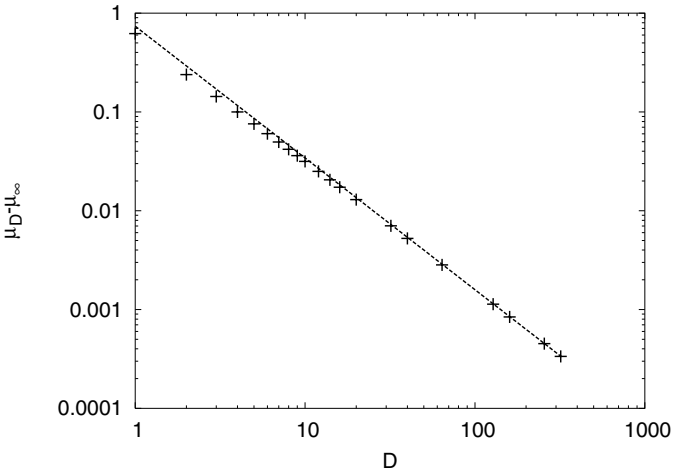

Fig. 3. Log-log plot of $\mu_D - \mu_\infty$ against D. The dashed line is $\mu_D - \mu_\infty = 0.737 D^{-1/\nu}$ with $\nu = 3/4$, as predicted by equation (3).

of course of dubious value for $d = 2$ (where it would give $B \approx 1.7$), but conformal invariance leads to the supposedly exact value $B = 2.01$ in $d = 2$ [3,4].

The monomer density is normalized such that $\sum_{y=1}^{D} \rho(y) = 1$. According to equation (9) it should scale as $y^{1/\nu}$ near the walls (this holds in any dimension) with $\nu = 3/4$. Surprisingly, we found that the simplest ansatz generalizing this power law to all $y \in [1, D]$,

$$\rho(y) = \frac{1}{D+1} f_\rho(\xi) \equiv \frac{1}{D+1} A(\xi(1-\xi))^{4/3} \; , \; \xi = \frac{y}{D+1} \; , \tag{10}$$

with $A = \Gamma(14/3)/\Gamma^2(7/3) = 10.38$ gives already an excellent fit (Fig. 4a) in the limit $D \to \infty$. There are small deviations invisible in Figure 4a but clearly seen when plotting $\rho(y)/f_\rho(\xi)$ (see Fig. 4b), but they seem to vanish slowly in the limit $D \to \infty$ (see Fig. 4b).

Assuming the latter, i.e. assuming that equation (10) becomes exact asymptotically, the universal number B could be estimated by using equations (1, 2, 3), and (9) which together would give

$$A = \lim_{D\to\infty} \lim_{y\to 0} \frac{D^{7/3}\rho(y)}{y^{4/3}} = \frac{4}{3}\frac{Ba}{k\mu_\infty} \; . \tag{11}$$

Inserting the above numbers gives $B = 2.122 \pm 0.002$ which is definitely larger than the value predicted in [3,4], by some 50 standard deviations.

In an alternative scenario we could assume that the deviations from equation (10) seen in Figure 4b do not vanish in the limit $D \to \infty$. In that case one should also allow for a modified scaling variable

$$\xi_\delta = (y - \delta)/(D + 1 - 2\delta) \tag{12}$$

with an unknown small (non-universal) parameter δ. Values of $(D + 1 - 2\delta)\rho(y)/f_\rho(\xi_\delta)$ for $D = 128$ and three different values of δ are plotted in Figure 4c. Similar results are obtained for other D. Combining them, we see

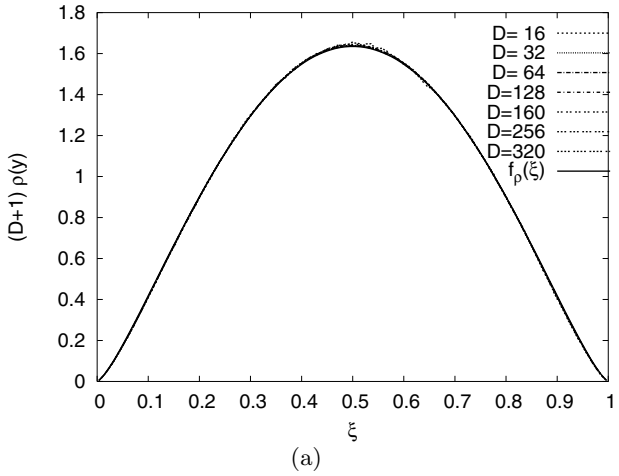

(a)

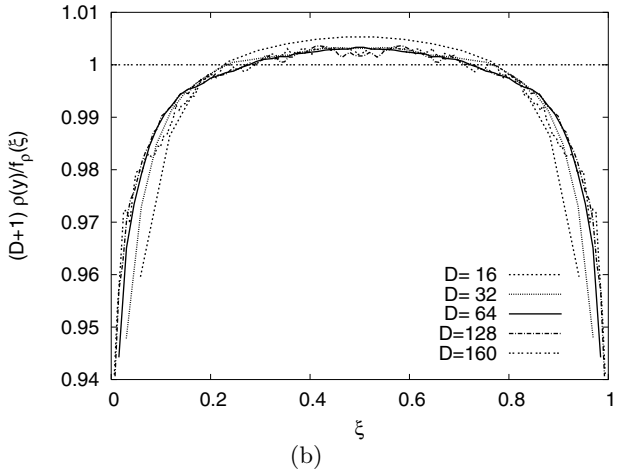

(b)

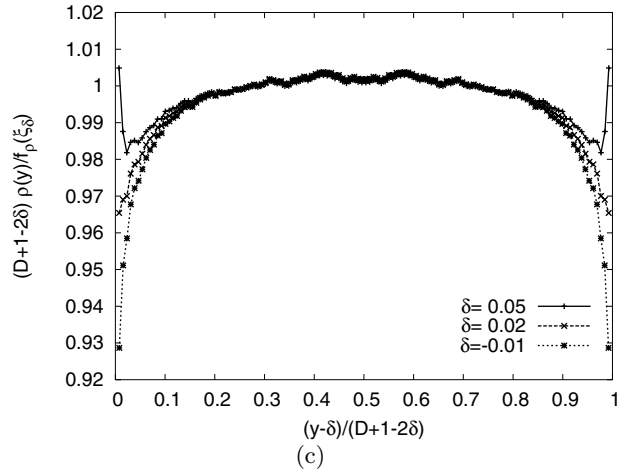

(c)

Fig. 4. (a) Rescaled values of the monomer density, $(D+1)\ \rho(y)$ against $\xi = y/(D+1)$. Also plotted is the function $f_\rho(\xi) = 10.38\ (\xi(1-\xi))^{4/3}$. (b) The same values (for $D \leq 160$), but divided by $f_\rho(\xi)$. In this panel we do not display our data for the largest lattices, since they are too noisy and would just blur the picture. They do however show the same trend as the data for $D \leq 160$. (c) The data for $D = 128$ plotted against a modified scaling variable, $\xi_\delta = (y-\delta)/(D+1-2\delta)$, divided by $f_\rho(\xi_\delta)$, for three different values of δ.

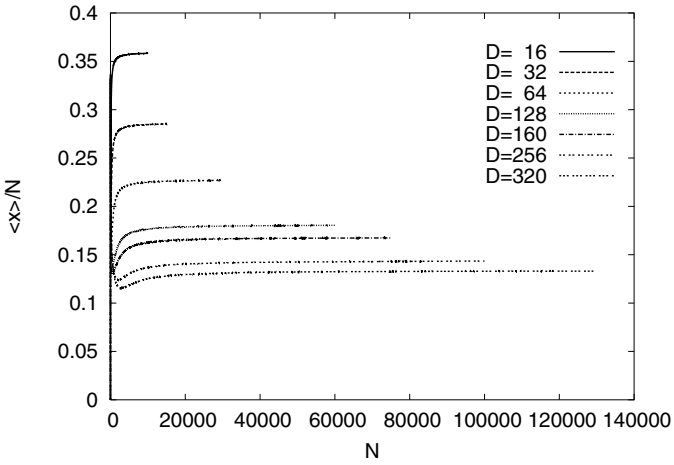

Fig. 5. End-to-end distance divided by N, $\langle x\rangle/N$, plotted against N for various values of D.

that best scaling (i.e. least dependence of D for small y) is obtained for $\delta \approx 0.02$. For this value of δ we have

$$\lim_{y\to 0,\ D\to\infty} D^{7/3}\rho(y)/y^{4/3} = (0.95 \pm 0.02) \times A\ . \qquad (13)$$

The large uncertainty in this estimate reflects the rather steep slope of the central curve in Figure 4c as $\xi_\delta \to 0$ and the related uncertainty in the best estimate of δ [24]. If we accept equation (13), we obtain $B = 2.04 \pm 0.04$, which is in perfect agreement with [3,4]. Thus we have two scenarios. Both imply very large corrections to scaling. While the a priori simpler scenario would be in conflict with the theoretical prediction, this prediction suggests that indeed the second scenario is correct, which is our preferred solution.

In Figure 5, we plot the end-to-end distance per monomer $\langle x\rangle/N$ versus N for various widths D. These curves become horizontal as $N \to \infty$, i.e. $\langle x\rangle$ increases indeed linearly with N, $\lim_{N\to\infty}\langle x\rangle/N = \Delta x$. In order to find how Δx scales with D, we plot it in Figure 6 on a doubly logarithmic scale. As indicated by the dashed line, it is fitted perfectly by the theoretical prediction [5]

$$\langle x\rangle/N \sim D^{1-1/\nu} = D^{-1/3}\ . \qquad (14)$$

We also estimated the density of wall contacts ρ_b (number of monomers at $y = 1$ or at $y = D$, divided by $2\langle x\rangle$). For each fixed value of D, this becomes independent of N as $N \to \infty$. The asymptotic values, obtained from plots similar to Figure 5, are also plotted in Figure 6. The full line corresponds to the very simple prediction [5]

$$\rho_b \sim D^{-2} \qquad (15)$$

which is independent of ν and indeed holds also for Gaussian chains. Equation (15) can be easily understood, in terms of the pressure exerted onto the wall:

$$\rho_b \sim p = \frac{Nf}{\langle x\rangle} \sim D^{-1-1/\nu+1/3} = D^{-2}\ . \qquad (16)$$

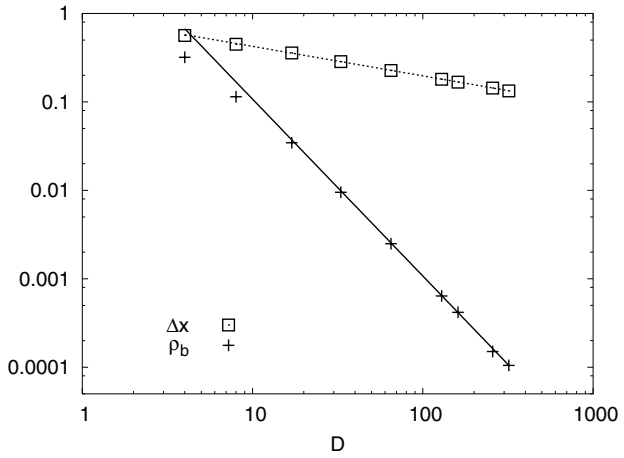

Fig. 6. Log-log plots of Δx and of the boundary density ρ_b versus D. The dashed line is 0.915 $D^{-1/3}$ and the solid line is 10.75 D^{-2}.

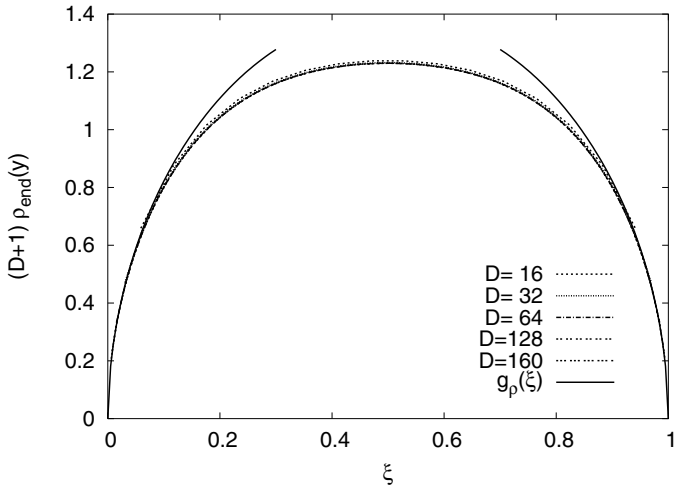

Fig. 7. Rescaled values of the probability $\rho_{end}(y)$ that the chain end is at the distance y from a wall against $\xi = y/(D+1)$. The topmost (interrupted) line is the function $g_\rho(\xi) = 2.85\ (\xi(1-\xi))^{25/48}$.

Finally, we show in Figure 7 the distribution $\rho_{end}(y)$ of chain ends. We see that $\rho_{end}(y)$ scales for large D (and for $N \gg D^{1/\nu}$, of course). Theoretically it is predicted that [23]

$$\rho_{end}(y) \sim y^{25/48} \tag{17}$$

for $y \ll D$. We see that this is indeed verified (the full lines in Figure 7 correspond to the prediction). But in contrast to the monomer density which was described fairly well for all y by the product of the power laws holding near the two walls, the same definitely does not hold for $\rho_{end}(y)$. There the function $g_\rho(\xi) = \text{const.}\ (\xi(1-\xi))^{25/48}$ does not describe the behaviour away from the walls.

4 Summary

We have shown that we could simulate 2-d polymers, modelled as self-avoiding walks, with chain length up to 125000 on strips of widths up to 320. This was possible using the PERM algorithm with Markovian anticipation. The fact that PERM gives by default very precise estimates of free energies allowed us to measure precisely the forces exerted onto the walls, by measuring how the critical fugacities depend on the width of the strips. We verified all critical scaling laws predicted for this problem, including the scaling of monomer and end point densities near the walls and the scaling of the total pressure with chain length and with strip width.

The only prediction for which we found possibly disagreement is for the universal amplitude ratio B defined in equation (9). A scenario based on some minimal assumption about scaling functions and corrections to scaling gives an estimate higher than the prediction by some fifty standard deviations. But a different scenario, maybe less plausible a priori but not very unlikely either, gives perfect agreement with the prediction. This illustrates again that one should be very careful about corrections to scaling, and that even very precise simulations do not always give unique answers when their analysis is not guided by a reliable theory.

Previous simulations of 3-d polymers between two parallel planar walls had indicated that also there the value of B might be larger than predicted, but those simulations had very large uncertainties. Using PERM we can simulate fairly easily much longer chains with rather high statistics. Results of such 3-d simulations will be given elsewhere.

We thank Profs. Erich Eisenriegler and Ted Burkhardt for valuable discussions, and Walter Nadler for carefully reading the manuscript.

References

1. P.G. de Gennes, *Scaling Concepts in Polymer Physics* (Cornell University Press, Ithaca, 1979)
2. E. Eisenriegler, *Polymers Near Surfaces* (World Scientific, Singapore 1993)
3. E. Eisenriegler, *Random walks in polymer physics*; in *Field Theoretical Tools in Polymer and Particle Physics*, edited by H. Meyer-Ortmanns, A. Klümper (Springer, Heidelberg, 1997)
4. J. Cardy, G. Mussardo, Nucl. Phys. B **410**, 451 (1993)
5. E. Eisenriegler, Phys. Rev. E **55**, 3116 (1997)
6. I. Webman, J.L. Lebowitz, M.H. Kalos, J. Phys. France **41**, 579 (1980)
7. T. Ishinabe, J. Chem. Phys. **83**, 423 (1985)
8. A. Milchev, K. Binder, Eur. Phys. J. B **3**, 477 (1998); **13**, 607 (2000)
9. J. De Joannis, J. Jimenez, R. Rajagopalan, I. Bitsanis, Europhys. Lett. **51**, 41 (2000)
10. R. Dickman, D.C. Hong, J. Chem. Phys. **95**, 4650 (1991)

11. P. Grassberger, Phys. Rev. E **56**, 3682 (1997)
12. P. Grassberger, H. Frauenkron, W. Nadler, *PERM: a Monte Carlo Strategy for Simulating Polymers and Other Things*, in *Monte Carlo Approach to Biopolymers and Protein Folding*, P. Grassberger et al. (World Scientific, Singapore, 1998), e-print `cond-mat/9806321` (1998)
13. H. Frauenkron, M.S. Causo, P. Grassberger, Phys. Rev. E **59**, R16 (1999)
14. S. Caracciolo, M.S. Causo, P. Grassberger, A. Pelissetto, J. Phys. A: Math. Gen. **32**, 2931 (1999)
15. M.N. Rosenbluth, A.W. Rosenbluth, J. Chem. Phys. **23**, 356 (1955)
16. P. Grassberger, unpublished
17. A.J. Guttmann, I.G. Enting, J. Phys. A **21**, L165 (1988)
18. A.R. Conway, A.J. Guttmann, Phys. Rev. Lett. **77**, 5284 (1996)
19. T.W. Burkhardt, I. Guim, Phys. Rev. E **59**, 5833 (1999)
20. J.E. Hopcroft, J.D. Ullman, *Introduction to Automata Theory, Languages, and Computation* (Addison-Wesley, Reading, 1979)
21. An analogous result holds for any regular language with m non-transient nodes in its minimal graph (or equivalently for a Markov source with m states): Markovian anticipation leads to weights which take on m different values, and thus no population control is needed to keep these weights within finite non-zero limits
22. B. Li, N. Madras, A.D. Sokal, J. Statist. Phys. **80**, 661 (1995)
23. J.L. Cardy, S. Redner, J. Phys. A: Math. Gen. **17**, L933 (1984)
24. Plotting $\rho(y)$ on a log-log plot would not help either. The large scale seen in Figure 4c implies that even the scaling exponent $1/\nu$ would be estimated wrongly from such a plot, unless one has much more complete data